7

Charge Transport in Carbon Nanotube Films and Fibers

Vitaly Ksenevich[1], Jean Galibert[2] and Vladimir Samuilov[1,3]
[1]*Belarus State University, Minsk*
Belarus
[2]*LNCMI & Universite de Toulouse*
France
[3]*State University of New York at Stony Brook*
USA

1. Introduction

Electrical properties and magnetotransport in carbon nanotubes (CNTs) have attracted much attention due to their importance in verification of existing theories of modern condensed matter physics and a number of possible applications (Robertson, 2007; Dai, 2002). Single-wall carbon nanotube (SWCNT) is a graphene sheet rolled up into a hollow cylinder and show metallic or semiconducting properties dependently upon their diameter and chirality. Due to their unique structure SWCNTs allows to study a large variety of different quantum phenomena like single-electron tunneling (Bockrath et al., 1997), Luttinger liquid behaviour (Bockrath et al., 1999), ballistic transport (Krstic et al., 2000), *etc*. Multi-wall carbon nanotubes (MWCNTs) are more complicated systems. They consist of a several shells of different diameter and chirality. Due to weak coupling between the shells the conductivity in bulk-contacted MWCNTs is defined mostly by the outermost shells. Diffusive transport in majority of experiments for individual MWCNTs was observed. Therefore quantum interference effects inherent for mesoscopic systems (weak localization and universal conductance fluctuation) were reported (Schonenberger et al., 1999). Besides that, MWCNTs with large diameter allows to observe Aahronov-Bohm effect at experimentally available values of magnetic fields (Bachtold et al., 1999; Lassagne et al., 2007). Ballistic transport even at room temperatures was observed by some authors (Frank et al., 1998; Urbina et al., 2003). Possibility to switch between ballistic and diffusive transport regime in the same MWCNTs sample using gate voltage by virtue of an electrostatic change of electron density was reported as well (Strunk et al., 2006; Nanot et al., 2009).
Processing of nanotubes on macroscopic scale and investigation of their synergetic properties is a most important task for realistic application of these materials, especially for fabrication of carbon nanotubes-based gas-, bio- and chemical sensors where signal from the sensor output depends on the conductivity of device (Stetter & Maclay, 2004). Different examples of morphology of the samples of arrays of nanotubes involve definitions of bundles (ropes) (Fischer et al., 1997; Krstic et al., 2000), mats (Fischer et al., 1997; Kaiser et al.,

1998), networks (Kim et al., 2001) and films (Baumgartner et al., 1997). The intertubes barriers and defects, length of the individual nanotubes in the assemblies as well as contact geometry play an essential role in the electrical transport properties of the carbon nanotube arrays. Therefore different charge transport mechanisms can be observed in the arrays of nanotubes: metallic conductivity, variable range hopping (VRH), weak localization (WL), and fluctuation induced tunneling. Combination of various mechanisms is possible as well. Verification of charge transport mechanisms (as well as the ranges of the temperature, electric and magnetic fields etc.) in which these mechanisms play dominating role is very important and non-trivial task for such systems.

In this chapter we show some examples of different CNTs assemblies in which contribution from different charge transport mechanisms can determine electrical properties of the systems. The chapter organized as follows. We briefly describe several methods of preparation of various types of CNTs assemblies (monolayers of MWCNTs and SWCNTs, SWCNTs fibers and SWCNTs coatings of silica fibers) and present experimental results on investigation of their transport properties. Besides traditional experimental technique used for investigations of charge transport (measurements of current-voltage *(I-V)* characteristics and resistance as a function of temperature and magnetic field), effect of the influence of strong microwave field and terahertz radiation on the conductivity of SWCNTs fibers and SWCNTs coatings of silica fibers was studied as well. Mechanisms responsible for the charge transport in CNTs assemblies were identified. Sensitivity of the electrical properties of carbon nanotubes arrays to the types of pristine carbon nanotubes, contacts geometry and to the preparation methods is considered. Special emphasize on the role of quality of intertube contacts in CNTs assemblies is done as a result of experimental data analysis.

2. Methods of preparation of carbon nanotubes arrays

2.1 Assembly of carbon nanotubes monolayers using Langmuir-Blodgett technique

Thin film geometry of CNT arrays is a most promising for their possible commercial applications like antistatic shielding and transparent conducting layers, if the layers are thin enough (Robertson, 2004), interconnections and heat sinks in integrated circuits, nano- and optoelectronic devices. However, assembly of CNTs into thin films or monolayers is hindered by processing and manipulations difficulties. The Langmuir-Blodgett (LB) technique can be used as a method for depositing of monolayers of molecularly ordered ultra-thin films with controlled thickness. However, due to absence of free bonds on the surface of nanotubes, they possess a high chemical stability and are insoluble in the organic solvents. Therefore, to find a possibility of arrangement of CNTs into arrays by means of LB technique, a chemical modification (functionalization) of their surfaces is necessary. Different approaches for CNTs functionalization were proposed, including covalent sidewall functionalization, noncovalent functionalization with surfactants and polymers, defect group functionalization and plasma modification of nanotubes sidewall (Bahr & Tour, 2002; Hirsch, 2002). One of the main advantage of the organic covalent functionalization of CNTs for their further assembly in thin films using LB technique is a possibility to obtain large surfaces covered by CNTs without free space. In contrast, quite low concentration of CNTs in layers was achieved when noncovalent functionalization was used (Krstic et al., 1998). Besides that, applications for chemical and biosensors may require the presence of different functional groups bounded to CNTs.

We used prior organic functionalization of MWCNTs based on the scheme described in (Georgakilas et al., 2002). The MCWNTs produced by chemical vapor deposition (CVD) method with catalyst 5%Fe,Co/CaCO3 with average diameter of about 30 nm and length less than 1 μm were used. The purified MWCNTs were suspended in DMF [N,N-Dimethylformamide HCON(CH3)2] together with an excess of *p*-Anisaldehide (4-methoxybenzaldehyde) CH3OC6H4CHO and 3-methylhippuric acid [m-toluric acid, N-(3-methyl-benzoyl)glycine] CH3C6H4CONHCH2CO2H. The heterogeneous reaction mixture was heated at 130 ^{o}C for approx. 120 hours. After the reaction was stopped, the organic phase was separated from unreached material by centrifugation and washing five times with chloroform ($CHCl_3$) and vacuum drying. The obtained dark solid phase was easily soluble in $CHCl_3$ up to a few mg/mL without sonication. The deposition of the layers (arrays) of nanotubes on the surface of the devices with the electrodes was done by using the cell, imitating the LB trough. Once a droplet of the solution of functionalized nanotubes in chloroform was spread on the water surface, a droplet of diblock-copolymer PS-PMMA solution was added in order to create a surface pressure of ~ 9 mN/m. The functionalized nanotubes were self-assembled in a dense arrays (monolayers) covering without free space the whole surfaces of the devices, when the monolayer was picked up from the water surface. The same procedure was done with grown by CVD method SWCNTs nanotubes. Scanning electron microscopy (SEM) image of dense arrays of SWCNTs is shown in Fig. 1.

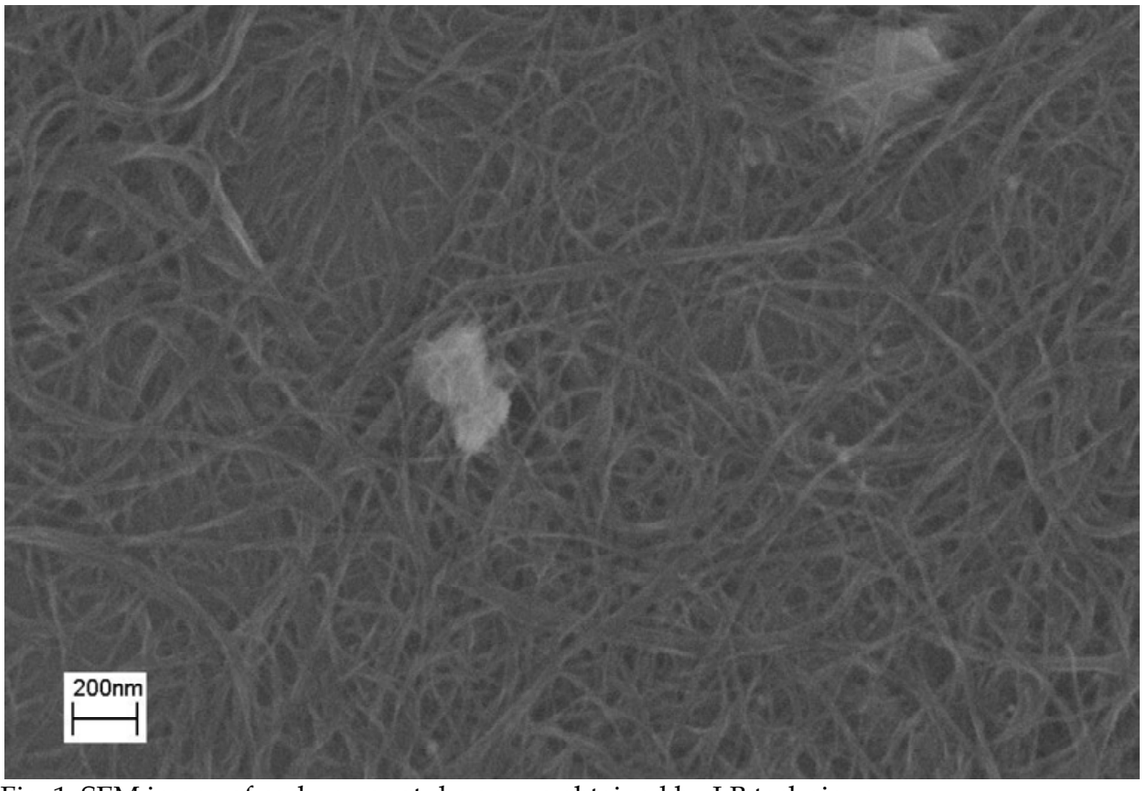

Fig. 1. SEM image of carbon nanotube arrays obtained by LB technique

Substrates with finger-shaped contact geometry with 10 μm distance between contacts were used for investigation of the electrical transport both for MWCNTs and SWCNTs arrays.

2.2 Preparation of SWCNTs fibers using wet-spinning process

Due to the high aspect ratio of the nanotubes and intertube coupling in conductivity of the arrays of carbon nanotubes, enhanced electrical transport properties are expected from the more aligned material. Therefore, different techniques for the alignment of nanotubes in the arrays are proposed: orientation of nanotubes in the films by using high magnetic fields (Smith et al., 2000), fabrication of fibers of aligned nanotubes by using an electrophoretic process (Gommans et al., 2000), synthesis of the fibers with the preferential nanotubes orientation by means of wet spinning process (Vigolo et al., 2000; Vigolo et al., 2002). The last technique can be potentially used for the large scale material production due to their particular simplicity and similarity to the industrial process of polymer fibers fabrication. We used SWCNTs fibers produced by polymer-free spinning method. The principle of the spinning method for the polymer/nanotubes composite fibers was reported in (Vigolo et al., 2000). The presence of non-conductive polymer poly vinyl alcohol (PVA) makes problematic the most applications of these fibers. Polymer-free SWCNTs fibers were produced in the process developed at Rice University (Davis et al., 2004; Zhou et al., 2004). The SWCNTs were dispersed in 102% sulfuric acid (2 wt. % excess SO_3) and then wet-spun into either diethyl ether 5% sulfuric acid, or water. The SWCNT fibers with high electrical and thermal conductivity were obtained using this technique. However, some protonation of material occurred due to long contact of fibers with sulfuric acid. Polymer-free SWCNTs fibers used in our experiments were synthesized without superacids from solutions comprising nanotubes, surfactant and water (Kozlov et al., 2005). SEM image of SWCNTs fiber produced by this method is shown in Fig. 2.

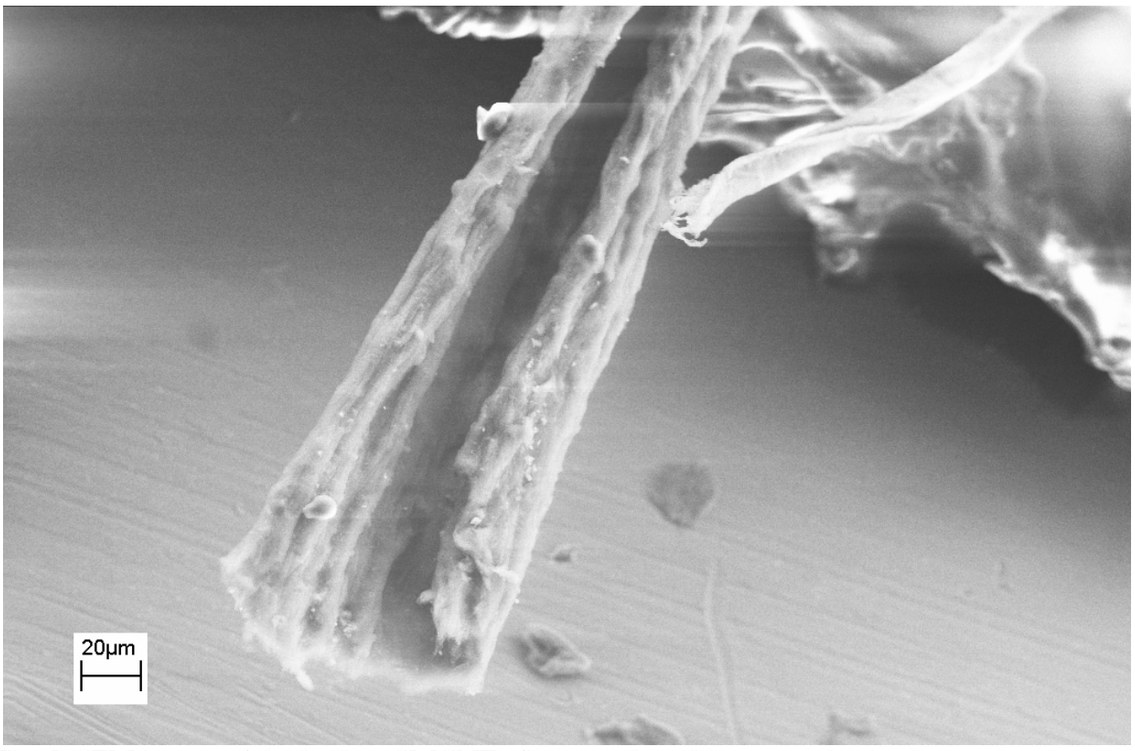

Fig. 2. SEM image of the hollow SWCNTs fiber produced by wet-spinning process

The nanotubes were dispersed using a horn sonicator in an aqueous solution of 1.2 wt.-% lithium-dodecyl-sulfate (LDS) surfactant. A narrow jet of this spinning solution was injected into the flocculation bath containing 37 % hydrochloric acid, which rotated at 33 rpm. The configuration of the rotating bath and spinneret needle was similar to that described for PVA-based coagulation spinning (Vigolo et al., 2000). Flocculation of nanotubes in the spinning solution to form a gel fiber occurred very close to the point of contact of the spinning solution and the acid in the bath. This gel fiber (containing 90 wt % volatilizable liquid, based on gravimetric measurements) was washed in methanol to remove the hydrochloric acid. The fiber, which has very low elasticity both before and after the washing step, was then pulled from the wash bath, stretched over a frame, and dried under tension. The fibers obtained by this method are of 20-100 μm diameter. As was mentioned above, one of the main advantages of this method for fabrication of the SWCNTs macroscopic arrays is the existence of the preferential orientation of individual nanotubes in the fibers due to flow-induced alignment of the nanotubes during processing (Vigolo et al., 2000). This alignment can be seen from the scanning electron microscopy (SEM) image of SWCNTs fiber shown in the Fig. 2.

SWCNTs with different geometry (solid, hollow and ribbon fibers) can be obtained by polymer-free wet spinning process in dependence of injection rate into the rotating bath of solution containing SWCNTs and inner spinneret diameter (Kozlov et al., 2005). HiPco SWCNTs obtained from a carbon monoxide process and SWCNTs prepared by laser ablation purchased from *Carbon Nanotechnologies Inc*. were used as pristine nanotubes for the SWCNTs fibers preparation. Electrical contacts for further measurements of charge transport in the fibers were made by Ag paint.

2.3 Fabrication of SWCNTs coatings of Silica fibers

Due to the high mechanical strength carbon nanotubes are widely used for reinforcement of different types composites materials, replacing conventional reinforcing fillers such as carbon or glass fibers (Shaffer & Sandler, 2007). Manufacturing of hierarchical composites with carbon nanotubes combined with conventional microscopic fibers has attracted growing interest years recently. Carbon nanotubes coatings on the surface of ceramic (Ci et al., 2005), carbon (Thostenson et al., 2002), quartz and aliminium silicate (Zhang et al., 2008) fibers were synthesized. Multi-wall carbon nanotubes coatings on the surface of silica fibers were obtained by chemical bonding (Liu et al., 2009) and using injection CVD method (Qian et al., 2009).

Procedure of preparation of SWCNTs coatings of silica fibers used in our investigations included the following stages: i) dissolving of polyimide claddings of silica fibers by soaking them in toluene for 2 hours, ii) cleaning of the residues of claddings by sonication in saturated KOH/propanol solution for 20 minutes with following sonication during 5 minutes in distilled water (this step was repeated several times), iii) silanization of silica fibers (creation of abundant carbon long alkyl chains on the silica fibers surfaces) in octadecyltrimethoxysilane (OTMS) solution in ethanol at a concentration of 2 mL/g for 2 hours. After that, the silanized silica fibers were soaked in water in which pristine SWCNTs were dispersed. When the silica fiber turns black due to a good coverage of SWCNTs as a result of clinging presumably driven by hydrophobic interactions, they were heated in an oven at 250^{o}C to anneal the bound SWCNTs. SEM image of SWCNTs coating on the surface of silica fiber obtained as a result of the above described procedure is shown in Fig. 3.

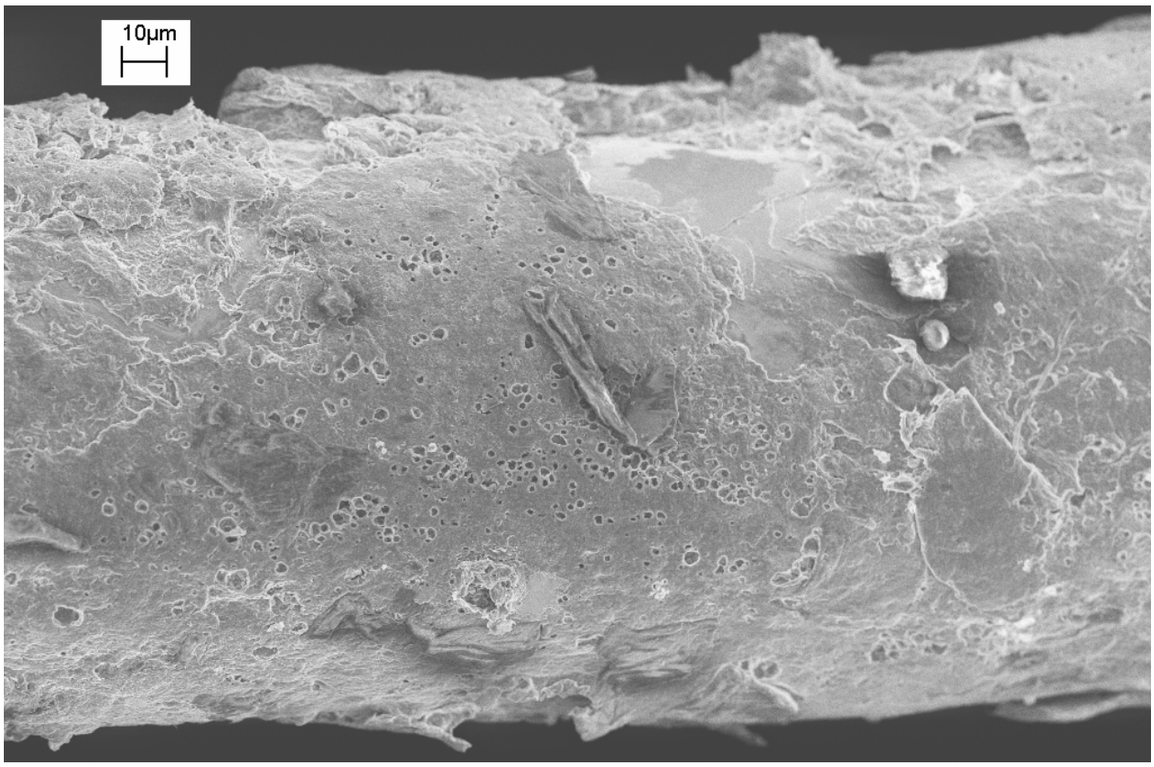

Fig. 3. SEM image of the side view of the silica fiber with good coverage of SWCNTs

For the further electrical and magnetotransport measurements silica fibers with SWCNTs coatings were transferred on solid substrates and electrical contacts were made by Ag paint.

3. Charge transport properties of carbon nanotubes arrays

3.1 Electrical and magnetotransport properties of carbon nanotubes monolayers

Measurements of the electrical and magnetotransport properties is one of the most reliable tool for exploring of different materials and verification of the mechanisms responsible for the charge transport in the system, (for a general revue of electronic and transport properties of carbon nanotubes, see (Charlier et al. 2007)). We used standard four-probe dc- and lock-in technique for the measurements of transport properties of carbon nanotubes assemblies in the temperature range 2-300 K. Magnetoresistance (MR) measurements were carried out in pulsed magnetic fields at the *Laboratoire National des Champs Magnētiques Intenses de Toulouse* (LNCMI) in the temperature range 2-300 K and up to 40 T magnitude fields.

We report and compare here the transport properties of different types of carbon nanotubes arrays. The temperature dependence of the resistance of the layers of short MWCNTs shows the negative temperature coefficient of the resistance ($dR/dT<0$) in the whole investigated temperature range (4.2-300 K) (Ksenevich et al., 2008 a) as one can see in the Fig. 4. Assuming possibility of the VRH conduction in our system due to structural defects and impurities, we fitted $R(T)$ dependence by classical law for variable range hopping (VRH) (Shklovskii & Efros, 1984):

$$R = R_0 \exp(T_0/T)^{1/n} \quad (1)$$

where $T_0=\beta/k_B\xi^3 g(\mu)$, β is a constant, k_B is a Boltzmann constant, ξ denotes the localization length, and $g(\mu)$ is the density of states, $n=d+1=2,3,4$ (d is the dimensionality of the system). In order to find parameter n we used both linearization in the scale $logR\text{-}T^{-1/n}$ and method proposed by Zabrodskii (Zabrodskii, 1977). We found that $R(T)$ dependence can be approximated by Eq. (1) in the temperature range T=4.2~60 K and the best fitting results were obtained at T below 60 K with parameter n=3, indicating 2D VRH.

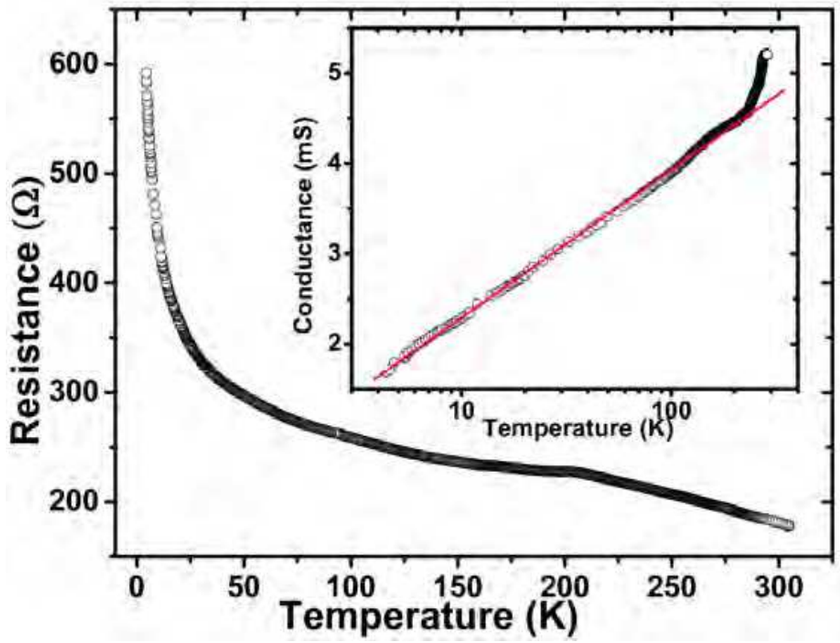

Fig. 4. The temperature dependence of the resistance of the MWCNTs arrays. The inset shows the $R(T)$ dependence in $G\text{-}LogT$ scale.

In order to see suitability of the WL theory for our system, we tried to fit $R(T)$ dependence with one-, two- and three-dimensional WL formulas. We found that $R(T)$ dependence follows the 2D weak localization (WL) behavior ($G(T)\sim lnT$) (Lee & Ramakrishnan, 1985) in the temperature range 4.2~202 K as one can see from the inset to Fig. 4 In the temperature range 202 - 300 K conductivity increases approximately linearly with temperature.

MR data measured at various temperatures are plotted in Fig. 5. The negative MR in the low magnetic fields range was observed. In the low-temperature range upturn of negative MR was observed. The minimum position of the negative MR shifts to the higher fields as the temperature rises. Both low-field negative MR due to changing of phase between alternate hopping paths enclosing a magnetic flux (Nguen et al., 1985; Sivan et al., 1988) and high-field positive MR due to electronic orbit shrinkage (Shklovskii & Efros, 1984) are predicted for systems with hopping conductivity mechanism. However, monotonic decrease of relative value of negative MR with the temperature rising are usually observed. In our samples the opposite situation is clearly seen: relative value of negative MR increased with the temperature rising in the low temperature range where VRH can be responsible for the

charge transport mechanism. From the other side negative MR is inherent for the systems where conductivity can be described in the frame of WL theory (Lee & Ramakrishnan, 1985).

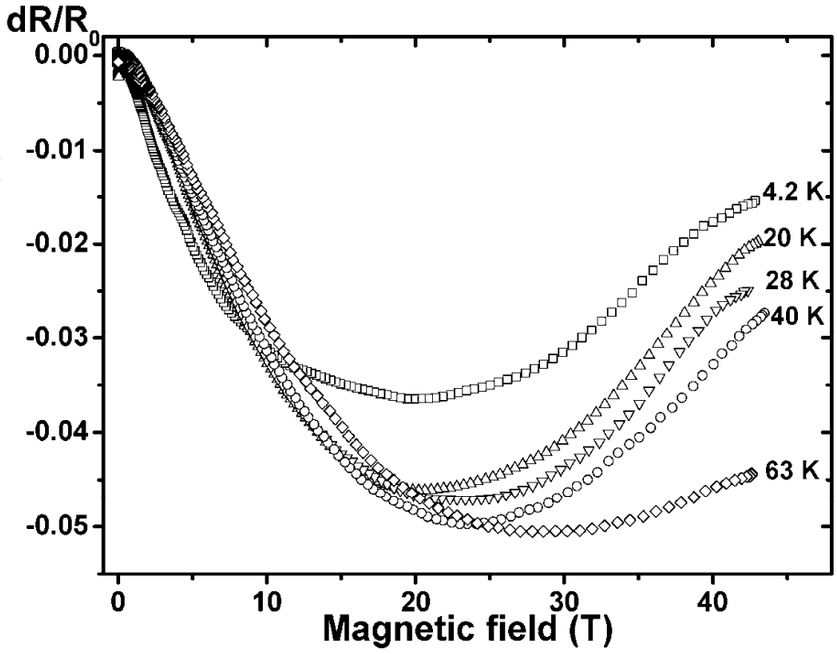

Fig. 5. The dependence of the normalized change in the resistance *dR/R(B=0)* of the MWCNTs arrays on the magnetic field in the temperature range 4.2 - 63 K.

Therefore we made assumption that MR data are the sum of the positive and negative contribution due to MR effects in the VRH and WL regimes, respectively. We found that high-field positive part of magnetoristance can be approximated in frame of Kamimura model for spin-dependent VRH conductivity (Kurobe & Kamimura, 1982):

$$\frac{\Delta G}{G} = -A_{KK}\frac{H^2}{H_{KK}^2 - H^2} \tag{2}$$

where $G=1/R$ is the conductance of the system, H_{KK} is the characteristic field for spin alignment, A_{KK} the saturation value of the magnetoconductance. Using formula (2) and values of parameters H_{KK} and A_{KK} obtained from the approximation data of high field MR data, we calculated positive magnetoresistance for low-field region. Pure negative contribution to MR according our assumption was calculated by subtracting positive MR from the experimental data. These data can be fitted reasonably well by the Eq. (3) for 2D WL:

$$\Delta G = \frac{e^2}{\pi h}[\psi(\frac{1}{2} + x) + \ln(x)] \tag{3}$$

where ψ is the digamma function, $x=L_{Th}^2 8\pi EH/hc$, $L_{Th} \sim T^{-p/2}$ is the Thouless length.

The example of the above mentioned procedure for extracting of positive and negative part from the total MR curve for temperature T = 40 K is shown in the Fig. 6.

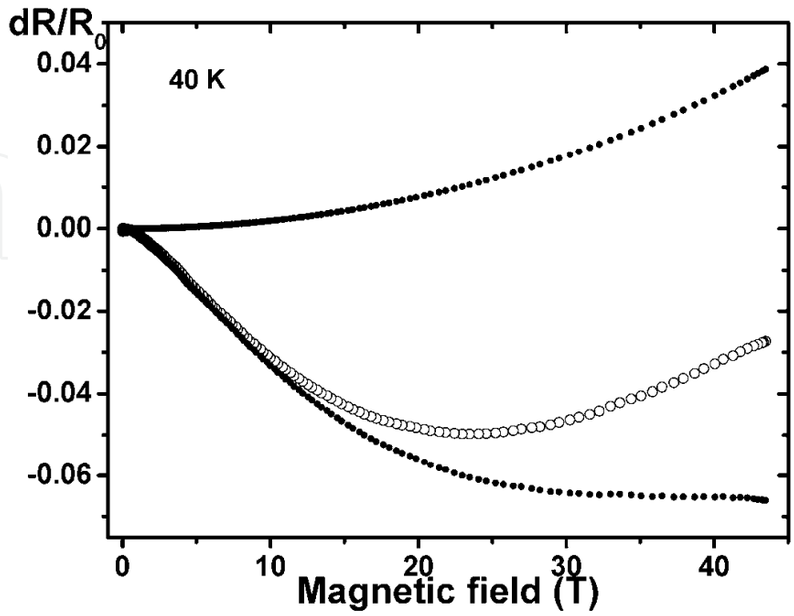

Fig. 6. The dependence of the normalized change in the resistance *dR/R(B=0)* of the MWCNTs arrays on the magnetic field measured at 40 K (open circle). Calculated value of positive MR obtained by fitting positive part of MR data to Eq. (2) (upper curve). The negative MR (lower curve) obtained by subtracting the calculated positive MR from the experimental MR data.

With this assumption we can explain positive upturn observed on MR curves by adding curves for positive and negative MR. Positive MR may come from the spin-dependent VRH among the defects on the surface of nanotubes. The negative contribution to MR can originate from the WL effects. It should be noted, that similar magnetotransport properties were observed for SWCNTs entangled networks (Kim et al., 1998). Therefore we can assume that similar MR effects in different type of carbon nanotubes arrays are defined not only by the type of pristine nanotubes, but their length and contact geometry as well. For both types of the samples the distance between contacts was much higher than the length of the separate nanotubes in the arrays, thus enhancing the probability to observe the localization effects.

Investigation of transport in SWCNTs monolayers confirms the importance of intertube contacts between separate nanotubes in their assemblies (Ksenevich et al., 2006). The temperature dependence of the resistance *R(T)* of the SWCNTs arrays is shown in Fig. 7.

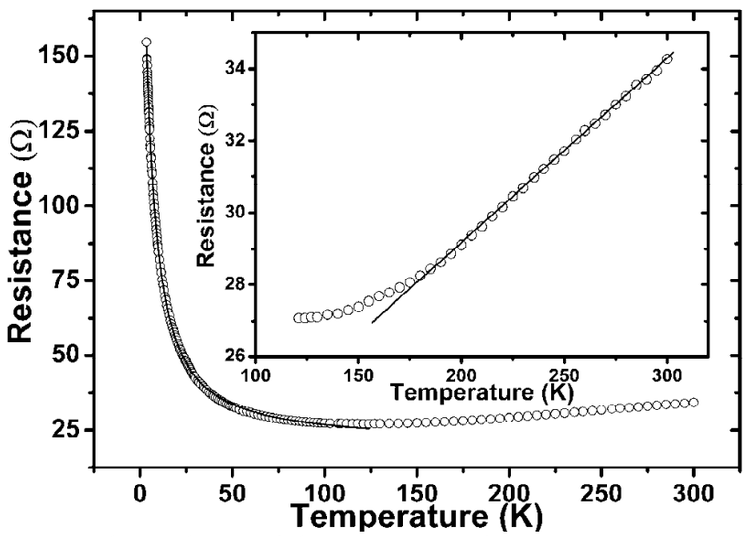

Fig. 7. The temperature dependence of the resistance of the SWCNTs arrays. Solid line is the fitting of the *R(T)* dependence by means of fluctuation-induced tunneling model (second term of Eq. (4)) in the low temperature range. The inset shows the high temperature metallic term of the *R(T)* dependence.

The resistivity minimum on the temperature dependence of the resistance of SWCNTs arrays was observed at *T*~125K. At *T*>125 K *R(T)* dependence has a metallic-type behavior (*dR/dT*>0) while in the low temperature range non-metallic sign for *R(T)* dependence (*dR/dT*<0) was observed. In the low-temperature range (*T* ~ 4.2 - 100 K) the temperature dependence of the resistance is consistent with the exponential law proposed for the fluctuation-induced tunneling model (Sheng, 1980). Thus, temperature dependence of the resistance can be written as:

$$R = \alpha T + R_t \exp(T_c/T+T_s), \quad (4)$$

where α is the temperature coefficient arising from metallic conductivity, and the second term represents the conductivity through the barriers between the metallic regions in frame of the fluctuation-induced tunnelling model. Such type of the temperature dependence of the resistance with systematic metallic sign and crossover to the non-metallic sign of the *R(T)* curves at lower temperatures was firstly observed by Fischer (Fischer et al., 1997) for SWCNTs ropes and mats. Heterogeneous model for conduction was proposed to explain crossover from metallic to non-metallic sign of the temperature dependence of the resistance as the temperature decreases (Kaiser et al., 1998). This model is based on the simple assumption that conduction process at high temperatures is defined by nanotubes with good metallic conductivity. The presence of small electrical barriers (tangled regions, intertube contacts, structural defects insight nanotubes itself) give rise to low temperatures localization effects. Therefore, the conductivity in the low temperature range is determined by tunneling through these electrical barriers. In our samples in the intermediate temperature range (*T* ~ 100 - 185 K) the contribution to the total conductivity of the system from the metallic conductivity and fluctuation-induced tunneling are comparable in the absolute value. This assumption explains the behavior of the *R(T)* dependence. Linear rise of

the resistance with temperature is clearly seen in the temperature range $T \sim 185 - 300$ K as one can see from the inset to Fig. 7. From the other side, due to a weak temperature dependence of the metallic term and its saturation at low temperatures of the temperature dependence the resultant resistance can be well fitted by fluctuation-induced tunneling law (second term of Eq. (4)).

It should be noted that the crossover temperature T between the metallic and nonmetallic type of $R(T)$ curve depends strongly on the type of SWCNTs arrays and quality of intertube contacts between separate nanotubes and varies from 35 K for a single well-ordered rope to 250 K for a rope with tangled regions (Fischer et al., 1997). Moreover, for SWCNTs with tangled regions the nonmetallic term can be described by proposed for variable range hopping conductivity Mott's law (1), indicating localization of charge carriers and hopping transport instead of fluctuation-induced tunneling (Kaiser et al., 1999). We assume that in our samples the localization effects and the resulting hopping transport can be essential only at very low temperatures where the rapid rise of the resistance is observed as the temperature decrease. This conclusion is confirmed by the shape of the MR curves, shown in Fig. 8.

Positive magnetoresistance with decreasing amplitude inherent for the variable range hopping conductivity was observed while temperature rising in the low temperature range. At temperatures higher than 7 K the MR effect is negligible. Because localization near defects is a possible cause of the barriers for charge carriers in heterogeneous conductivity model, magnetoresistance can exhibit localization effects at low temperatures, inducing positive MR. However absolute value of the positive magnetoresistance can be lower in comparison with uniformly disordered systems as far as the conductivity in our heterogeneous system is enhanced by the well conductive metallic regions (metallic carbon nanotubes).

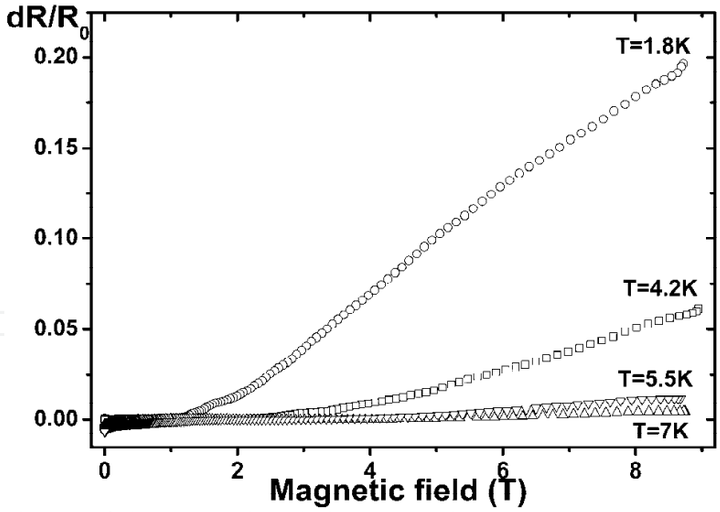

Fig. 8. The dependence of the normalized change in the resistance $dR/R(B=0)$ of the SWCNTs monolayers on the magnetic field in the temperature range 1.8-7 K.

3.2 Charge transport in SWCNTs fibers

Electrical and thermal transport properties of the SWCNT fibers fabricated by means of wet spinning process in correlation with the orientation degree of nanotubes inside fibers are already reported (Zhou et al., 2004; Badaire et al., 2004). For the optimizing of conducting

properties of SWCNT fibers for possible applications deeper understanding of the charge transport mechanism in this material is required.

We applied different experimental techniques in order to study transport properties of SWCNTs fibers and to distinguish mechanisms responsible for the charge carrier's transfer in the system (Ksenevich et al., 2008 b; Ksenevich et al., 2008 c). We have measured resistance as a function of temperature and magnetic field, current-voltage (*I-V*) characteristics, and investigated effect of the influence of the strong microwave field and terahertz radiation on the conductivity of SWCNT fibers. The *R*(*T*) dependence of the SWCNT fibers is shown in Fig. 9. In the low-temperature range (4.2 - 80 K) the resistance as a function of temperature exhibits a classical VRH conduction, following the law (1) with exponent $n=4$, assuming 3D character of hopping conductivity. In the temperature range T = 80 - 300 K $R(T)$ dependence can be approximated by a typical law for fluctuation-induced tunneling conductivity mechanism (Sheng, 1980):

$$R = R_t \exp(T_c/T+T_s), \tag{5}$$

where parameters T_c and T_s are defined by the following equations:

$$T_s = 16\varepsilon_0 \hbar A V_0^{3/2}/(\pi e^2 k_B (2m_e)^{1/2} w^2, \tag{6}$$

$$T_c = 8\varepsilon_0 A V_0^2/(e^2 k_B w), \tag{7}$$

where w is the width of the tunnel junction, A labels its area, and V_0 is the height of the contact potential; k_B stands for the Boltzmann constant, $\hbar$ is a Plank constant, e is the electronic charge, m_e the electron's effective mass, and ε_0 the vacuum permittivity.

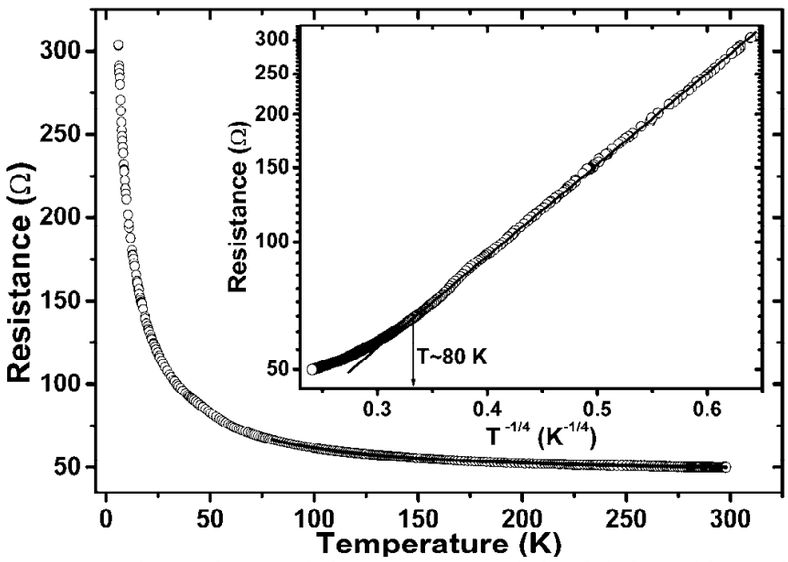

Fig. 9. The temperature dependence of the resistance of the SWCNT fibers. Solid line is the fitting of the *R(T)* dependence by means of fluctuation-induced tunneling model in the temperature range 80 - 300 K. The inset shows the logR-$T^{-1/4}$ plot. (According to ref. (Ksenevich et al., 2008 b)).

Fluctuation-induced tunneling conductivity model was proposed for disordered heterogeneous systems contrary to the systems with hopping charge carrier transport between localized sites. These systems (for example, conductor-insulator composites, granular metals, disordered semiconductors) consist of large conductive segments (where electrons are delocalized and free to move over very large distances as compared to the atomic dimensions) separated by small insulating gaps. Due to small sizes of tunnel junction, thermal voltage fluctuation resulting from the thermal motion of electrons in the conduction region in the vicinity of tunnel barrier can change drastically the electron tunneling probability through the barrier. Different types of carbon nanotubes arrays with existing electrical barriers can be also considered as heterogeneously disordered systems. Therefore this model was used for describing the temperature dependence of conductivity of SWCNTs fibers (Zhou et al., 2004) and networks (Kim et al., 2001). As was mentioned earlier we observed fluctuation induced tunneling conductivity in the low temperature range for SWCNTs layers obtained by LB technique. As one can see from Fig. 9 for our SWCNTs fibers the fitting results also agree well with experimental data thus indicating the importance of intertube contacts between individual carbon nanotubes. Assuming the area A of the tunnel junction being equal to the cross section of a SWCNT with the diameter of about 1.5 nm and using expressions for parameters T_c and T_s, the effective junction width is estimated to be 4.6 nm and the effective barrier height to be 0.172 eV.

I-V curves of SWCNTs fibers measured in the temperature range 6 – 300 K are plotted in Fig. 10. At room temperature, linear *I-V* curves were observed. As the temperature decreases, the non-Ohmic behavior becomes pronounced. Nonlinearity of *I-V* curves is clearly seen at temperatures about 100 K and becomes more significant in the low temperature range. Reproducibility of the *I-V* curves by number of thermal cycling and different sweeping times indicate that the heating effect is negligible. Nonlinear *I-V* characteristics for both charge transport mechanisms (VRH and fluctuation induced tunneling) can be observed.

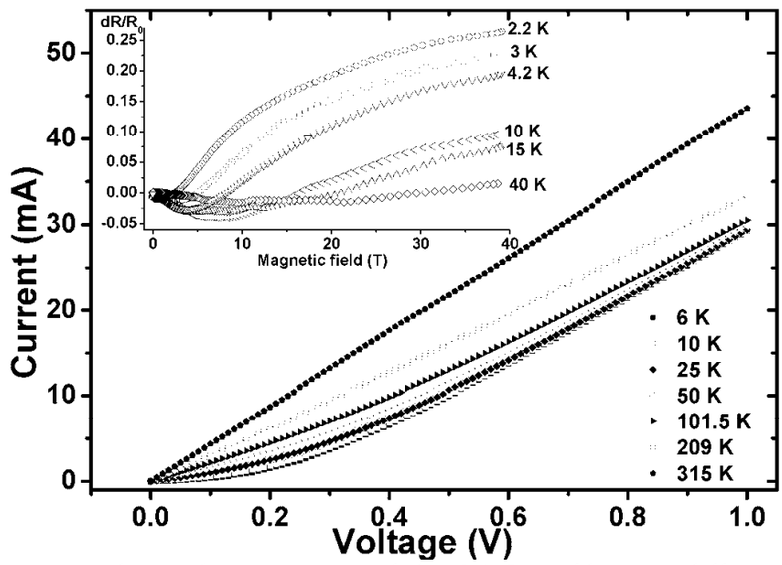

Fig. 10. The current-voltage characteristics of the SWCNT fibers at different temperatures. The inset figure: the dependence of the normalized change in the resistance *dR/R(B=0)* of the SWCNTs fibers on the magnetic field in the temperature range 2.2-40 K (According to ref. (Ksenevich et al., 2008 b)).

As far as $R(T)$ dependencies in the low temperature range were approximated by Mott's law (1) for VRH conductivity, we assumed that nonlinearity of the I-V curves can be explained within the framework of classical theoretical models for hopping conductivity (Pollak & Riess, 1976; Grannan et al., 1992). According to these models, in the low electric fields, the conductivity is expected to be nearly independent of the applied electric field. In this regime hopping of the charge carriers between hopping sites is induced by phonons. In the high electric fields, both temperature and electric fields (with energy scales k_BT and eEl, respectively, where E is the electric field and l is the length parameter related to maximum hopping length between the hopping sites) have similar activation effects on the charge carriers. Low fields are defined as fields $E<Ec$, where $Ec=k_BT/el$. In the region of high electric fields $Ec<E<k_BT/e\xi$ (where ξ is a localization length), non-Ohmic VRH conductivity follows the formula (Pollak & Riess, 1976; Grannan et al., 1992):

$$\sigma(E,T) = \sigma(0,T)\exp(eUl/k_BTd), \tag{8}$$

where U is the voltage measured between voltage probes and d is the distance between them. However, we found rather large discrepancies between experimental data and fitting curves in the region of very high electric field ($E>k_BT/e\xi$) where theoretical models for VRH predict "activationless" conductivity. In this regime charge carriers acquire the energy necessary for hopping between localized sites not from the phonons but from the electric field, and the conductivity becomes temperature independent: $\sigma(E) \sim exp(-E_0/E)^m$, where the exponent m is usually equal to exponent in formula (1) for the Ohmic regime of hopping conductivity as was found in most experiments. Therefore in order to check the possibility to explain the origin of nonlinearity of I-V curves in the frame of the VRH models, we estimated the fitting parameter $(k_Bd/el)T$ at different temperatures from the slope of $ln(U)$ dependencies. From the slope $log(k_Bd/el)T$ versus $logT$ we obtained the temperature dependence of the parameter l (maximum hopping length), $l \sim T^{0.13}$. This means that hopping length slightly increases with the temperature, and this fact contradicts to the classical VRH models. As it was mentioned above, in the low temperature range, the $R(T)$ dependencies of the SWCNT fibers measured in the linear range of I-V curves were fitted well by Mott's law (1). According to the Mott's model for 3D VRH, the maximum hopping length can be described as $l \sim T^{-0.25}$. Therefore, the nonlinearity of I-V curves cannot be explained by the influence of the high electric fields on the hopping conductivity. We assume that at $T<80$ K, where $R(T)$ dependencies are well fitted by Mott law (1), the VRH conductivity can be considered as the charge transport mechanism in the SWCNT fibers only for low electric fields $E<Ec$. We found that best fitting results of the nonlinear IV curves in the whole range of applied electric fields can be obtained by using the extended Sheng's model (Sheng, 1980) proposed by Kaiser and Park (Kaiser & Park, 2005):

$$G = I/V = G_0\exp(V/V_0)/(1+h[\exp(V/V_0 -1)]) \tag{9}$$

where G_0 is the temperature dependent low-field conductance, parameter V_0 is the voltage scale factor that gives an exponential increase in conductance and depends strongly on the barrier energy, and parameter $h=G_0/G_h$, where G_h reflects the large conductance in the absence of barriers. Eq. (9) was obtained by means of numerical calculations of fluctuation induced tunneling and thermal activation (Kaiser & Park, 2005).

We carried out also measurements of the dependence of the resistance on the magnetic field in order to clarify the charge transport picture in SWCNT fibers. The general features of MR at different temperatures behavior can be seen from the insert to Fig. 10.

At low fields, MR is negative. A positive upturn is observed on the MR curves, of which position is shifted to higher magnetic field as the temperature increases. The upturn field of the MR effect was shifted from 1.5 T at 2 K to value of about 20 T at 40 K. The value of positive MR varies as $exp(B^2)$ which changes to $exp(B^{1/3})$ behavior at sufficiently high fields as expected for the VRH transport (Shklovskii & Efros, 1984). The tendency to saturation of the positive MR was observed at low temperatures as one can see from the inset to Fig. 10. However, the negative MR can not be explained in frame of Sivan model (Sivan et al., 1980) proposed for VRH charge transport. According to this model the negative MR should saturate when one flux quantum $\Phi_0=hc/e$ penetrates an area equal $R_M^{3/2}\chi^{1/2}$ (here R_M - the average hopping length and χ - the average distance between the localization centers). The position of the negative MR minimum shifts to the higher fields with increasing temperature due the hopping length decrease and as a consequence, an area bounded by different paths decreases. In addition, the monotonic decrease of the relative value of negative MR with the temperature is usually observed. We found the nonmonotonic behavior of the relative value of the negative MR with the temperature. At T=2 K the relative value of the negative MR was about 0.4 %. The maximum of the relative negative MR value about 4.2 % was observed at T=10 K. At the further temperature increasing the negative MR decreases. Therefore, the contribution of the other mechanism must be considered in order to explain the negative MR behavior. One of the possible explanations of the negative MR can be a contribution of the weak localization effects in total MR (Lee & Ramakrishnan, 1985).

The determined carrier transport features were supported by additional measurements of the change in conductivity in strong 10 GHz microwave fields and measurements of THz radiation induced photocurrent at various lattice temperatures.

Relaxation kinetics of the THz induced photovoltage at different temperatures are shown in Fig. 11. In order to diminish Joule heating of the samples due to absorption of laser radiation pulsed THz radiation with low repetition rate (30 Hz) and duration of pulses of 100 μs (the shortest possible pulse available in this kind of optically-pumped molecular terahertz laser) was used. Two relaxation processes are visible: relatively fast part (with time constant of some hundreds of μs which corresponds to the duration of THz pulses) and relatively slow part (in the range of about ~20 ms) that we associate with the Joule heating. The fast peak we associate with the influence of terahertz radiation on the hopping conductivity. We assume this effect as *terahertz - induced hopping conductivity* (Ksenevich et al., 2008 b), taking into account the following arguments. In the low temperature range where VRH conduction is observed, the conductivity increases with temperature because of activation of charge carriers by thermal energy k_BT on hopping sites located at higher energy levels. Since the terahertz radiation energy is in the order of magnitude of thermal energy (1 THz ~ 4 meV ~ 48 K), that terahertz quanta exceeding the thermal energy k_BT should give rise to additional increase of conductivity. On the other hand, within the temperature rise fluctuation induced tunneling mechanism starts to prevail. As it is evident from the experiments, it becomes negligible at T~30 K. Only slow Thz – induced signal due to heating is observed. We assume that contributions from fluctuation induced tunneling and VRH at this temperature are comparable on the absolute value of magnitude.

The dependencies of the variation of the conductivity of SWCNT fibers on applied microwave field power at the temperatures 77 and 300 K measured using technique described in (Pozela, 1985) are shown in the inset to Fig. 11.

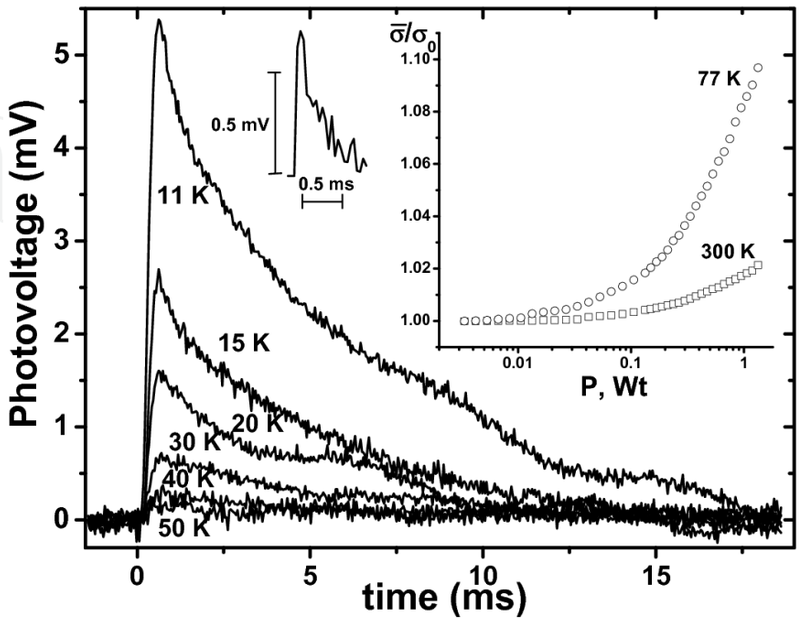

Fig. 11. Relaxation kinetics of THz-induced photovoltage signal at different temperatures. Left inset: terahertz induced photocurrent transient excluding lattice heating. In the right inset the dependence of the conductivity variation on applied microwave power is shown. (According to ref. (Ksenevich et al., 2008 b)).

The increase of the conductivity on microwave power becomes more essential with the temperature decrease as one can see from the right inset to Fig. 11. At the same microwave field power of about 1 W the observed value of relative conductivity increase was about 2 % and 10 % at the temperatures 300 K and 77 K, respectively. It should be noted that the heating of the charge carriers by strong microwave field can give rise to conductivity both in VRH and fluctuation-induced tunneling regimes due to a possible rising of the probability of charge carriers for the hopping between the localized sites and for the tunneling through the barriers, respectively.

3.3 Conductivity mechanisms in SWCNTs coatings of Silica fibers

According to our knowledge the electrical transport in SWCNTs coatings of silica fibers had not been studied earlier.

We used a standard dc 4-probe technique for measurements of the electrical and magnetotransport properties of the SWCNTs-SiO_2 coatings in a close-cycled cryostat in the temperature range 1.8-300 K and in the magnetic fields up to 8 T (Ksenevich et al., 2009). Charge transport in the system was found to have general features similar to the properties of SWCNTs fibers produced by polymer-free wet spinning process. The *R(T)* dependence of the SWCNTs coatings of silica fibers can be well fitted by a typical law (5) for fluctuation-induced tunneling model (Sheng, 1980) almost in the whole range of temperatures

(~8-300 K). The best fit to Eq. (5) was obtained with parameters T_s=13.3 K and T_c=52.8 K. Assuming that the area A of the tunnel junction equals to the cross section of a SWCNT with diameter of about 1.5 nm and using equations (6) and (7) for parameters T_s and T_c, the effective junction width was estimated to be 3.2 nm and the effective barrier height of 68 meV. In the low temperature range (2~8 K) *R(T)* dependence was found to follows the Mott law (1) for 3D variable range hopping (VRH) conduction (Shklovskii & Efros, 1984). It should be noted that both for SWCNTs fibers and SWCNTs coatings of silica fibers non-metallic sign for *R(T)* dependence (dR/dT<0) was observed in the whole range of temperatures in contrast to SWCNTs monolayers. We believe that possibility to observe metallic sign for *R(T)* dependence for SWCNTs fibers and SWCNTs coatings of silica fibers is hindered by large distance between contacts (about ~ 1 *mm*) in contrast to SWCNTs monolayers, where length of pristine nanotubes exceeded distance between contacts (10 *μm)* in finger-shaped structures.
Magnetoresistance data measured at different temperatures are shown in Fig. 12.

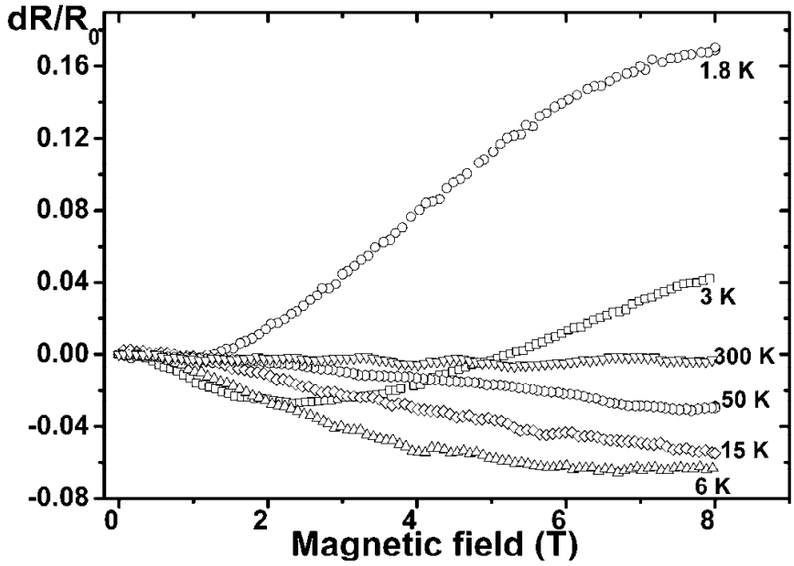

Fig. 12. The dependence of the normalized change in the resistance *dR/R(B=0)* of the SWCNTs coatings of silica fibers on the magnetic field in the temperature range 1.8 - 300 K.

Both positive and negative MR was observed in the temperature range 1.8 - 6 K. The value of positive MR varies as $exp(B^2)$ as expected for the VRH transport and explained by electronic wave function shrinkage in the magnetic field. Tendency to saturation of positive MR was observed at 1.8 K at the value of magnetic field higher than 6 T. Non-monotonic behavior of relative value of negative MR was observed similar to the experimental data for MR of SWCNTs fibers. The relative value of negative MR increases with temperature in the range of 1.8-6 K. As the temperature exceeds 6 K, only negative MR is observed in the available range of magnetic fields, and the relative value of negative MR then decreases as the temperature rises. One can note, however, that in order to extract the negative contribution to the total magnetoresistance and to clarify the physical origin of this negative MR, a further analysis is needed both for SWCNTs fibers and SWCNTs coatings of SiO_2 fibers.

The experiments in strong microwave field in GHz range and THz radiation-induced photocurrent measurements were carried out as well in order to get an additional view into the electrical transport phenomena in SWCNTs coatings of silica fibers in comparison with transport properties of SWCNTs fibers.

The relaxation kinetics of photocurrent recorded at 1.6 THz frequency measured at different temperatures are shown in Fig. 13. Similar to the THz radiation-induced photocurrent experiments carried out for SWCNTs fibers the relaxation kinetics allows one to distinguish two different processes: relatively fast (with time constant of about of some hundreds of μs, which corresponds to the duration of THz pulses) due to terahertz-induced hopping conductivity, and slow (with time constant in the range of *ms*) due to the Joule heating of the samples. The decreasing of the amplitude of the fast photocurrent signal with the temperature was observed. Quantitative differences between the experimental results on the measurements of the conductivity under THz radiation for SWCNTs coatings of silica fibers and for SWCNT fibers were observed. Firstly, the amplitude of fast photocurrent signal is higher at the same temperatures and at the same frequency of THz radiation for the SWCNTs coatings of silica fibers. Secondly, the time constant for slow part of photocurrent signal is several times lower for SWCNTs-SiO_2 samples than for SWCNT fibers. Thz radiation-induced photocurrent measurements allow us to assume that in the intermediate temperature range both charge transport mechanism (VRH and fluctuation induced tunneling) can coexist. Therefore, the first difference can be explained by the higher degree of alignment of carbon nanotubes in fibers due to specifics of wet spinning method (Kozlov et al., 2005) and as a consequence a higher contribution to the total conductivity of VRH transport in comparison with SWCNTs fibers. A possible reason of lower duration of slow photocurrent signal component in SWCNTs coatings of silica fibers can be the heat exchange between the silica core and SWCNTs coatings.

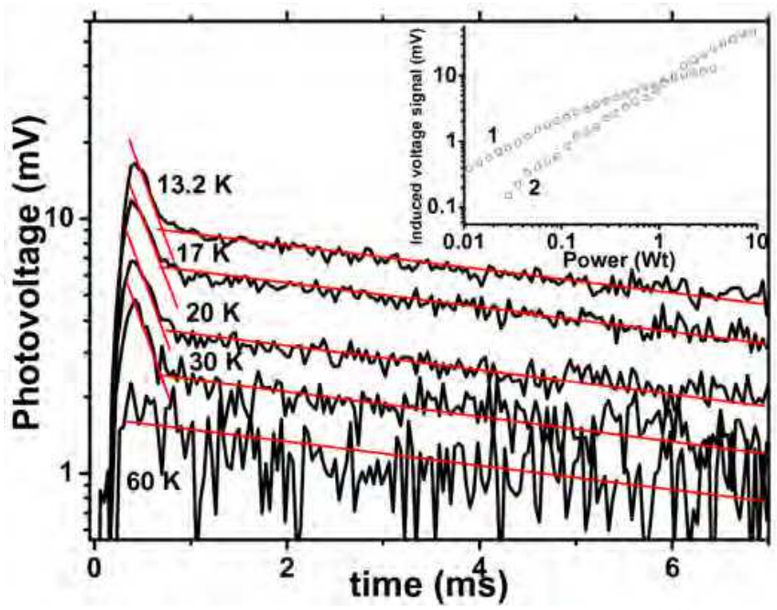

Fig. 13. Terahertz radiation-induced photocurrent at 1.6 THz at different temperatures in SWCNTs coatings of silica fibers. In the inset induced voltage signal proportional to the change of conductivity as function of microwave power at liquid nitrogen temperature for SWCNTs fibers (curve 1) and SWCNTs coatings of silica fibers (curve 2) is shown.

Measurements of the conductivity change of SWCNTs coatings of silica fibers in strong microwave field of 10 GHz at 77 and 300 K have shown similar results with experiments carried out for the SWCNTs fibers produced by wet spinning process. We observed increase in conductivity in microwave fields became more pronounced lowering the temperature. The data measured at 77 K are plotted in the inset to Fig. 13. For comparison, results both for SWCNTs fibers and SWCNTs coatings of silica fibers are given. As one can see, for both types of structures, the dependence is similar, however in SWCNTs-SiO_2 it follows a linear law while for SWCNTs fibers it becomes sublinear with microwave power.

As was mentioned above, heating of charge carriers by strong microwave field can give rise to conductivity both in VRH and fluctuation-induced tunneling regimes. However, according to the *R(T)* dependencies we can assume that the fluctuation-induced tunneling is a prevailing mechanism of charge carrier transport at 77 K for both types of samples. Hence, the difference in transport properties can be only defined by the barrier height. This can be an argument to explain the more rapid increase of conductivity with microwave fields in SWCNT-SiO_2 samples containing lower effective barrier height in comparison to that of SWCNTs fibers (68 meV *vs* 172 meV).

4. Conclusion

Electrical and magnetotransport properties of various types of carbon nanotubes arrays were reported. Different fabrication procedures for assembly of separate carbon nanotubes into monolayers, SWCNTs fibers and coatings of silica fibers were used. Langmuir-Blodgett (LB) technique was applied for self-assembling of SWCNTs and MWCNTs monolayers. SWCNTs fibers were synthesized using wet spinning process from solutions comprising nanotubes, surfactant and water. SWCNTs coatings were produced by means of clinging of pristine SWCNTs dispersed in water to previously silanized silica fibers. We experimentally showed that the electrical and magnetotransport properties of investigated carbon nanotubes arrays are defined not only by the types of pristine carbon nanotubes (multi wall or single wall with different chiralities) but also by the quality of intertube coupling between separate nanotubes from which these assemblies consist of.

Magnetotransport properties of MWCNTs arrays can be interpreted in framework of model assuming existing of two charge transport mechanisms in the system: spin-dependent hopping conductivity and 2D weak localization.

Charge transport properties of 2D arrays of SWCNTs can be interpreted in terms of heterogeneous model for conduction where the presence of structural defects and intertube connections give rise to low temperature localization effects. The conductivity of the system at high temperatures is determined by the charge transport trough metallic nanotubes.

Experimental data for SWCNTs fibers and SWCNTs coatings of silica fibers could be consistent both with the charge transport model for homogeneously disordered materials due to low-temperature localization of charge carriers arising from the defects in the tubes themselves and with the model for heterogeneous materials that emphasizes the role of energy barriers between the nanotubes.

Acknowledgments

We highly appreciate Mikhail Kozlov, David Novitski, Robin Helburn and Qi Lu for sample preparations and Gintaras Valusis, Dalius Seliuta, Irmantas Kasalynas and Zigmas Martunas for providing possibility and kind assistance in microwave and THz experiments and for useful discussions.

5. References

Bachtold, A.; Strunk, C.; Salvetat, J.-P.; Bonard, J.-M.; Forro, L.; Nussbaumer, T. & Schonenberger, C. (1999). Aharonov-Bohm oscillations in carbon nanotubes. *Nature,* Vol. 397, No. 6721, pp. 673-675

Badaire, S.; Pichot, V.; Zakri, C.; Poulin, P.; Launois, P.; Vavro, J.; Guthy, C.; Chen, M. & Fischer, J. E. (2004). Correlation of properties with preferred orientation in coagulated and stretch-aligned single-wall carbon nanotubes. *J. Appl. Phys.*, Vol. 96, No. 12, pp. 7509–7513

Bahr, J.L. & Tour, J.M. (2002). Covalent chemistry of single-wall carbon nanotubes. *J. Mater. Chem.,* Vol. 12, No. 7, pp. 1952–1958

Baumgartner, G.; Carrard, M.; Zuppiroli, L.; Bacsa, W.; de Heer, W. A. & Forro, L. (1997). Hall effect and magnetoresistance of carbon nanotube films. *Phys. Rev. B*, Vol. 55, No. 11, pp. 6704-6707

Bockrath, M.; Cobden, D. H.; McEuen, P. L.; Chopra, N. G.; Zettl, A.; Thess, A. & Smalley, R. E. (1997). Single-Electron Transport in Ropes of Carbon Nanotubes. *Science*, Vol. 275, No. 5308, pp. 1922-1925

Bockrath, M.; Cobden, D. H.; Lu, J.; Rinzler, A. G.; Smalley, R. E.; Balents, L. & McEuen, P. L. (1999). Luttinger-liquid behavior in carbon nanotubes. *Nature*, Vol. 397, No. 6720, pp. 598–601

Charlier, J.-C.; Blase, X. & Roche, S. (2007). Electronic and transport properties of nanotubes *Rev. Mod. Phys.*, Vol. 79, No. 2, pp. 677-732

Ci, L. J.; Zhao, Z. G. & Bai, J. B. (2005). Direct growth of carbon nanotubes on the surface of ceramic fibers. *Carbon*, Vol. 43, No. 4, pp. 883–886

Dai, H. (2002). Carbon nanotubes : opportunities and chalenges. *Surface Science*, Vol. 500, No. 1-3, pp. 218–241

Davis, V. A.; Ericson, L. M.; Parra-Vasques, A. N. G.; Fan, H.; Wang, Y.; Prieto, V.; Longoria, J. A.; Ramesh, S.; Saini, R. K; Kittrell, C; Billups, W. E.; Adams, W. W.; Hauge, R. H; Smalley, R. E. & Pasquali, M. (2004). Phase Behavior and Rheology of SWNTs in Superacids. *Macromolecules,* Vol. 37, No. 1, pp. 154-160

Fischer, J. E.; Dai, H.; Thess, A.; Lee, R.; Hanjani, N. M.; Dehaas, D. L. & Smalley, R. E. (1997). Metallic resistivity in crystalline ropes of single-wall carbon nanotubes. *Phys. Rev. B*, Vol. 55, No. 8, pp. R4921-R4924

Frank, S.; Poncharal, P.; Wang, Z. L. & De Heer, W. (1998). Carbon Nanotube Quantum Resistor. *Science*, Vol. 280, No. 5370, pp. 1744-1746

Georgakilas, V.; Kordatos, K.; Prato, M.; Guldi, D.M.; Holzingeer, M. & A. Hirsch. (2002). Organic Functionalization of Carbon Nanotubes. *J. Am. Chem. Soc.,* Vol. 124, No. 5, pp. 760-761.

Gommans, H. H.; J. Alldredge, W.; Tashiro, H.; Park, J.; Magnuson, J. & Rinzler, A. G. (2000). Fibers of aligned single-walled carbon nanotubes: Polarized Raman spectroscopy. *J. Appl. Phys.,* Vol. 88, No. 5, pp. 2509-2514

Grannan, S. M.; Lange, A. E.; Haller, E. E. & Beeman, J. W. (1992). Non-Ohmic hopping conduction in doped germanium at T<1K. *Phys. Rev. B,* Vol. 45, No. 8, pp. 4516-4519.

Hirsch, A. (2002). Functionalization of Single-Walled Carbon Nanotubes. *Angew. Chem. Int. Ed.*, Vol. 41, No. 11, pp. 1853-1859

Kaiser, A. B.; Dusberg, G. & Roth, S. (1998). Heterogeneous model for conduction in carbon nanotubes. *Phys. Rev. B*, Vol. 57, No. 3, pp. 1418–1421

Kaiser, A. B.; Park, Y. W.; Kim. G. T., Choi, E. S.; Dusberg, G. & Roth, S. (1999). Electronic transport in carbon nanotube ropes and mats. *Synth. Met.*, Vol. 103, No. 1-3, pp. 2547–2550

Kaiser, A. B. & Park, Y. W. (2005). Current-voltage characteristics of conducting polymers and carbon nanotubes. *Synth. Met.,* Vol. 152, No. 1- 3, pp. 181-184

Kim, G. T.; Choi, E. S.; Kim, D. C.; Suh, D. S..; Park, Y. W.; Liu, K.; Dusberg, G. & Roth, S. (1998). Magnetoresistance of an entangled single-wall carbon-nanotube networks. *Phys. Rev. B*, Vol. 58, No. 24, pp. 16064–16069

Kim, G. T.; Jhang, S. H.; Park, J. G.; Park, Y. W. & Roth, S. (2001). Non-ohmic current-voltage characteristics in single-wall carbon nanotube networks. *Synth. Met.*, Vol. 117, No. 1–3, pp. 123–126

Kozlov, M. E.; Capps, R. C.;W. Sampson, M.; Ebron, V. H.; Ferraris, J. P. & Baughman, R. H. (2005). Spinning Solid and Hollow Polymer-Free Carbon Nanotubes Fibers. *Adv. Mater.,* Vol. 17, No. 5, pp. 614-617

Krstic, V.; Duesberg, G.S.; Muster, J.; Burghard, M. & Roth, S. (1998). Langmuir-Blodgett Films of Matrix-Diluted Single-Walled Carbon Nanotubes. *Chem. Mater.*, Vol. 10, No. 9, pp. 2338-2340

Krstic, V.; Roth, S. & Burghard, M. (2000). Phase breaking in three-terminal contacted single-wall carbon nanotube bundles. *Phys. Rev. B*, Vol. 62, No. 24, pp. R16353-R1635

Ksenevich, V. K.; Galibert, J.; Forro, L. & Samuilov, V. A. (2006). Magnetotransport in 2D-arrays of single-wall carbon nanotubes, In: *Carbon Nanotubes: From Basic Research to Nanotechnology,* NATO ASI Series II: Mathematics, Physics and Chemistry, Vol.222, Popov, V. N. & Lambin, P. (Eds.), pp. 183–184, Springer, ISBN 978-1-4020-4572-1, Dordrecth, The Netherlands

Ksenevich, V. K.; Aboltin, R. S.; Dauzhenka, T. A., Galibert, J. & Samuilov, V. A. (2008, a). Charge transport mechanisms in the arrays of multi-walled carbon nanotubes, *Proceedings of the III International conference Materials and structures of modern electronics*, pp. 271-273, ISBN 978-985-518-091-4, Minsk, Belarus, September, 2008, BSU publishers, Minsk

Ksenevich, V.K.; Odzaev, V.B.; Martunas, Z.; Seliuta, D.; Valusis, G.; Galibert, J.; Melnikov, A.A.; Wieck, A.D.; Novitski, D.; Kozlov, M.E. & Samuilov, V.A. (2008, b). Localization and nonlinear transport in single walled carbon nanotube fibers. *J. Appl. Phys.*, Vol. 104, No. 7, pp. 073724-1–073724-7

Ksenevich, V.K.; Seliuta, D.; Martunas, Z.; Kasalynas, I.; Valusis, G.; Galibert, J.; Kozlov, M.E. & Samuilov, V.A. (2008, c). Charge Carrier Transport Properties in Single-Walled Carbon Nanotube Fibers. *Acta Phys. Pol. A,*, Vol. 113, No. 3, pp. 1043–1046

Ksenevich, V.; Dauzhenka, T.; Seliuta, D.; Kasalynas, I.; Kivaras, T.; Valusis, G.; Galibert, J.; Helburn, R.; Lu, Q. & Samuilov, V.A. (2009). Electrical transport in carbon nanotubes coatings of silica fibers. *Physica Status Solidi (c),* Vol. 1-3, DOI 10.1002/pssc.200982553 (in press).

Kurobe, A. & Kamimura, H. (1982). Correlations Effects on Variable Range Hopping Conduction and the Magnetoresistance. *J. Phys. Soc. Jap.,* Vol. 51, pp. 1904-1913

Lassagne, B.; Cleuziou, J.-P.; Nanot, S.; Escoffer, W.; Avriller, R.; Rosche, S.; Forro, L.; Raquet, B. & Broto, J.-M. (2007). Aharonov-Bohm Conductance Modulation in Ballistic Carbon Nanotubes. *Phys. Rev. Lett.,* Vol. 98, No. 17, p.p. 176802-1-176802-4

Lee, P. & Ramakrishnan, T.V. (1985). Disordered electronic systems. *Rev.Mod.Phys.,* Vol. 57, No. 2, pp. 287-337.

Liu, H.; Li, J.; Liu, X. & Jiang, S. (2009). A novel multiwalled carbon nanotubes bonded fused-silica fiber for solid phase microextraction–gas chromatographic analysis of phenols in water samples. *Talanta,* Vol. 78, No. 3, pp. 929–935

Nanot, S.; Escoffier, W.; Lassagne, B.; Broto, J.-M. & Raquet, B. (2009). Exploring the electronic band structure of individual carbon nanotubes under 60 T. *C. R. Physique,* Vol. 10, No. 4, pp. 268-282

Nguen, V. L., Spivak, B. Z. & Shklovskii, B. I. (1985). Tunnel hopping in a disordered systems. *Sov. Phys. JEPT,* Vol. 62, No. 5 , pp. 1021-1029

Qian, H.; Bismarck, A.; Greenhalgh, E. S. & Shaffer, M. S. P. (2010). Synthesis and characterisation of carbon nanotubes grown on silica fibres by injection CVD. *Carbon,* Vol. 48, No. 1, pp. 277–286

Pollak, M. & Riess, I. (1976). A percolation treatment of high-field hopping transport. *J. Phys. C*, Vol. 9, No. 12, pp. 2339–2352

Pozela, J. K. (1985). Transport parameters from microwave conductivity and noise measurements, In: *Topics of Applied Physics*, L. Reggiani (Ed.), Vol. 58, pp. 113–147, Springer-Verlag, Berlin

Robertson, J. (2004). Realistic applications of CNTs. *Materials Today*, Vol. 7, No. 10, pp. 46-52

Robertson, J. (2007). Growth of nanotubes for electronics. *Materials Today*, Vol. 10, No. 1-2, pp. 36–43

Schonenberger, C.; Bachtold, A.; Strunk, C.; Salvetat, J.-P. & Forro, L. (1999). Interference and Interaction in multi-wall carbon nanotubes. *Appl. Phys. A,* Vol. 69, No. 3, pp. 283-295

Shaffer, M. & Sandler, J. (2007). Carbon nanotube/nanofibre polymer composites, In: *Processing and properties of nanocomposites,* Advani, S. G., (Ed.), pp. 1–59, World Scientific, ISBN: 978-981-270-390-3, New Jersey, NJ

Sheng, P. (1980). Fluctuation-induced tunneling conduction in disordered materials. *Phys. Rev. B*, Vol. 21, No. 6, pp. 2180–2195

Shklovskii, B. I. & Efros, A. L. (1984). *Electronic properties of doped semiconductors,* Springer, ISBN-10: 0387129952, Berlin, New York

Sivan, U.; Entin-Wohlman, O. & Imry, Y. (1988). Orbital Magnetoconductance in the Variable-Range-Hopping Regime. *Phys. Rev. Lett.,* Vol. 60, No. 15, pp. 1566-1569

Smith, B. W.; Benes, Z.; Luzzi, D. E.; Fischer, J. E. ; Walters, D. A.; Casavant, M. J.; Schmidt, J. & Smalley, R. E. (2000). Structural anisotropy of magnetically aligned single wall carbon nanotube films. *Appl. Phys. Lett.,* Vol. 77, No. 5, pp. 663–665

Stetter, J. R. & Maclay, G. J. (2004). Carbon Nanotubes and Sensors: a Review. In: *Advanced Micro and Nanosystems*, Vol. 1, Baltes, H.; Brand, O.; Fedder, G.K.; Hierold, C.; Korvink, J.G. & Tabata, O. (Eds.), pp. 357–382, Wiley-VCH Verlag GmbH & Co, ISBN-13: 978-3-527-30746-3, Weinheim, Germany

Strunk, C.; Stojetz, B. & Roche, S. (2006). Quantum interference in multiwall carbon nanotubes. *Semicond. Sci. Technol,* Vol. 21, No. 11, pp. S38–S45

Thostenson, E. T.; Li, W. Z.; Wang, D. L.: Ren, Z. F. & Chou, T. W. (2002). Carbon nanotube/carbon fiber hybrid multiscale composites. *J. Appl. Phys.,* Vol. 91, No. 9, pp. 6034–6037

Urbina, A.; Echeverria, I.; Perez-Garrido, A.; Diaz-Sanchez, A. & Abellan, J. (2003). *Phys. Rev. Lett.,* Vol. 90, No. 10, pp. 106603-1-106603-4

Vigolo, B.; Penicaud, A.; Coulon, C.; Sauder, C.; Pailler, R.; Journet, C.; Bernier, P. & Poulin, P. (2000). Macroscopic Fibers and Ribbons of Oriented Carbon Nanotubes. *Science,* Vol. 290, No. 5495, pp. 1331–1334

Vigolo, B.; Poulin, P.; Lucas, M.; Launois, P. & Bernier, P. (2002). Improved structure and properties of single-wall carbon nanotube spun fibers. *Appl. Phys. Lett.,* Vol. 81, No. 7, pp. 1210–1212

Zabrodskii, A. G. (1977). Hopping conduction and density of localized states near the Fermi level. *Soviet Phys. Semicond.,* Vol. 11, pp. 345-348

Zhang, Q.; Qian, W.; Xiang, R.; Yang, Z.; Luo, G.; Wang Y, & Wei, F. (2008). In situ growth of carbon nanotubes on inorganic fibers with different surface properties. *Mater. Chem. Phys.,* Vol. 107, No. 2-3, pp. 317–321

Zhou, W.; Vavro, J.; Guthy, C.; Winey, K. I.; Fischer, J. E.; Ericson, L. M.; Ramesh, S.; Saini, R.; Davis V. A.; Kittrel, C.; Pasqualli, M.; Hauge, R. H. & Smalley, R. E. (2004). Single wall carbon nanotube fibers extruded from super-acid suspensions: Preferred orientation, electrical, and thermal transport. *J. Appl. Phys.,* Vol. 95, No. 2, pp. 649-655

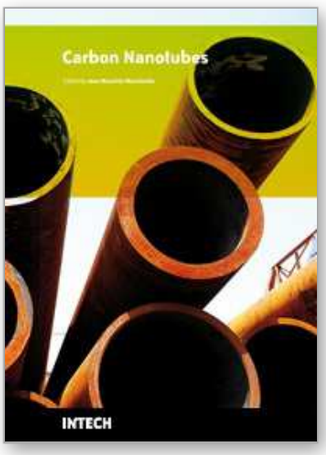

Carbon Nanotubes

Edited by Jose Mauricio Marulanda

ISBN 978-953-307-054-4
Hard cover, 766 pages
Publisher InTech
Published online 01, March, 2010
Published in print edition March, 2010

This book has been outlined as follows: A review on the literature and increasing research interests in the field of carbon nanotubes. Fabrication techniques followed by an analysis on the physical properties of carbon nanotubes. The device physics of implemented carbon nanotubes applications along with proposed models in an effort to describe their behavior in circuits and interconnects. And ultimately, the book pursues a significant amount of work in applications of carbon nanotubes in sensors, nanoparticles and nanostructures, and biotechnology. Readers of this book should have a strong background on physical electronics and semiconductor device physics. Philanthropists and readers with strong background in quantum transport physics and semiconductors materials could definitely benefit from the results presented in the chapters of this book. Especially, those with research interests in the areas of nanoparticles and nanotechnology.

INTECH
open science | open minds

InTech Europe
University Campus STeP Ri
Slavka Krautzeka 83/A
51000 Rijeka, Croatia
Phone: +385 (51) 770 447
Fax: +385 (51) 686 166
www.intechopen.com

InTech China
Unit 405, Office Block, Hotel Equatorial Shanghai
No.65, Yan An Road (West), Shanghai, 200040, China
中国上海市延安西路65号上海国际贵都大饭店办公楼405单元
Phone: +86-21-62489820
Fax: +86-21-62489821

IntechOpen